Appl. Phys. B 77, 633–637 (2003)
DOI: 10.1007/s00340-003-1272-x

**Applied Physics B**
**Lasers and Optics**

S.D. GEORGE✉
P. RADHAKRISHNAN
V.P.N. NAMPOORI
C.P.G. VALLABHAN

# Photothermal deflection studies on heat transport in intrinsic and extrinsic InP

International School of Photonics, Cochin University of Science and Technology, Kochi 682 022, India

**Received: 17 March 2003/Revised version: 10 June 2003**
**Published online: 30 September 2003 •** 

**ABSTRACT** Laser induced transverse photothermal deflection technique has been employed to determine the thermal parameters of InP doped with Sn, S and Fe as well as intrinsic InP. The thermal diffusivity values of these various samples are evaluated from the slope of the curve plotted between the phase of photothermal deflection signal and pump-probe offset. Analysis of the data shows that heat transport and hence the thermal diffusivity value, is greatly affected by the introduction of dopant. It is also seen that the direction of heat flow with respect to the plane of cleavage of semiconductor wafers influences the thermal diffusivity value. The results are explained in terms of dominating phonon assisted heat transfer mechanism in semiconductors.

**PACS** 78.20.Nv; 66.30.Xj; 61.72.Vv

## 1 Introduction

InP is a very important compound semiconductor, which finds wide applications in the realms of the electronic and optoelectronic industry, especially as a substrate material in optical fiber communication and in the fabrication of heterostructure lasers [1, 2]. The thermal properties of this material merit close scrutiny from a device fabrication point of view. The heat diffusion in such materials is essentially determined by thermal diffusivity value [3, 4], the inverse of which is a measure of the time required to establish thermal equilibrium in the specimen in which a transient temperature change has occurred [5]. As the doping can alter the characteristics of these semiconductors, a detailed investigation of influence of doping on thermal diffusivity value is of great physical and practical significance. Moreover, the influence of cleavage plane on the thermal diffusivity value is also very important as it has profound applications in the growth of quantum wells and superlattices. A detailed investigation on the influence of doping and the plane of cleavage on the heat transport and hence on the thermal diffusivity in a nondestructive manner are of great significance, especially for the proper modeling of devices based on these semiconductors.

✉ Fax: +91-484/2576714, E-mail: sajan@cusat.ac.in

In the recent years, thermal wave physics has been emerging as an effective research and analytical tool for the characterisation of thermal, transport and optical properties of matter in all its different forms [6–8]. The laser induced nondestructive and nonintrusive photothermal methods are widely used for the thermal characterisation of materials, particularly for the evaluation of the thermal diffusivity value [9, 10]. All the photothermal methods are based on the detection, by one means or other, of a transient temperature change that characterizes the thermal waves generated in the sample after illumination with a chopped optical radiation [11]. In spite of a variety of photothermal methods used for the characterisation of materials, the noncontact photothermal deflection (PTD) technique possesses some unique characteristics and advantages compared to other photothermal methods [5, 7, 12]. The PTD technique can be employed in various configurations depending on the nature of the specimen under investigation, such as the collinear photothermal deflection technique and transverse photothermal deflection technique or the so-called mirage technique [13]. The PTD technique is essentially based on the detection of the refractive index gradient associated with a temperature gradient induced within the specimen [14].

In this paper, the thermal characterisation of intrinsic InP and InP doped with Sn, S and Fe is described. Among the various experimental approaches for evaluating the thermal diffusivity of semiconductors using PTD, the strategy that used in the present investigation is the measurement of the PTD signal as a function of pump-probe offset [7, 13].

## 2 Theory

A variety of detection configurations can be employed for the thermal and optical characterisation of material using the PTD technique [14, 15]. Amongst these, the skimming PTD technique is the simplest and the most popular approach for the thermal characterisation of materials. The details of this configuration are explained elsewhere [16]. In the skimming PTD configuration the specimen is irradiated with a chopped and focused laser radiation and the subsequent periodic nonradiative de-excitation of the specimen produces periodic thermal waves. These periodic thermal waves create refractive index variation in the coupling medium (usually a liquid with high $\mathrm{d}n/\mathrm{d}T$ value), which is in contact with

the specimen. A low power probe beam skimming through the sample surface is used to monitor this refractive index gradient. The nature of the refractive index gradient is essentially dependent on the parameters of the specimen under investigation. Thus the probe beam, which is passing through a spatially varying refractive index gradient, suffers deflection from its normal path and the measurement of this deflection allows the characterization of the thermal and optical parameters of the specimen under investigation [17, 18].

For a Gaussian probe beam propagating through an inhomogenous medium, most of the parameters can be deduced from the analysis made by Mandelis and Royce [19]. The propagation of a guassian beam through a spatially varying refractive index is given by the expression

$$\frac{\mathrm{d}}{\mathrm{d}s}\left(n_0\frac{\mathrm{d}r_0}{\mathrm{d}s}\right)=\nabla_{\perp}n\,(r,t)\ , \tag{1}$$

where $r_0$ is the perpendicular displacement of the beam from its original direction. $n_0$ is the uniform index of refraction and $\nabla_{\perp}n\,(r,t)$ is the gradient of index of refraction perpendicular to the ray path. (1) can be integrated over the ray path:

$$\frac{\mathrm{d}r_0}{\mathrm{d}s}=\frac{1}{n_0}\int\limits_{\text{path}}\nabla_{\perp}n\,(r,t)\ \mathrm{d}s\,, \tag{2}$$

where $s$ is the optical path length. Because the deviation is small, one can write the deflection $\Phi(t)$ as

$$\frac{\mathrm{d}r_0}{\mathrm{d}s}=\Phi\,(t)=\frac{1}{n_0}\frac{\partial n}{\partial T}\int\limits_{\text{path}}\nabla_{\perp}T\,(r,t)\ \mathrm{d}s\,, \tag{3}$$

where $\nabla_{\perp}T\,(r,t)$ is the temperature gradient perpendicular to the ray path. Deflection $\Phi(t)$ can be resolved into two components $\Phi_n$ and $\Phi_t$, which are, respectively, the deflections normal and parallel to the sample surface. If the probe beam make a transverse offset $y$ with respect to the pump beam axis and a vertical offset $z$ with respect to the sample surface, then the temperature field distribution that is due to the pump beam absorption, obtained by the solution of the heat diffusion equations in the sample as well as in the coupling fluid, leads to the evaluation of $\Phi_n$ and $\Phi_t$ as

$$\Phi_n=-\frac{1}{\pi n}\frac{\mathrm{d}n}{\mathrm{d}t}\int\limits_0^{\infty}\cos(\delta y)\,A\exp(-\beta_0 z)\,\beta_0\,\mathrm{d}\delta\exp(j\omega t)$$

$$\text{for } z>0 \tag{4}$$

and

$$\Phi_t=-\frac{1}{\pi n}\frac{\mathrm{d}n}{\mathrm{d}t}\int\limits_0^{\infty}\sin(\delta y)\,A\exp(-\beta_0 z)\,\delta\,\mathrm{d}\delta\exp(j\omega t)$$

$$\text{for } z>0 \tag{5}$$

where $A$ is a complex integration constant and $\delta$ is a spatial Fourier transformed variable and

$$\beta_0=\left(\delta^2+\frac{j\omega}{D_0}\right)^{\frac{1}{2}}\ ,$$

where $D_0$ is the thermal diffusivity of the coupling liquid.

A linear relationship between the PTD signal phase as well as amplitude with various parameters such as pump-probe offset and height of the probe beam above the sample surface has already been reported [17]. For $a=b=z=0$, where $a$, $b$, $z$ are the pump beam spot size, probe beam spot size and the probe beam height above the sample surface, there is a linear relation between the phase of the PTD signal and the pump-probe offset. This linear relation is found to be applicable in three different configurations of pump and probe:

1. probe beam skimming configuration with pump and probe on the same side of the sample,
2. probe beam skimming configuration with pump and probe on the different sides of the sample,
3. probe beam passing through the sample.

The first configuration is used for the present investigation. In this configuration, the slope of the plot connecting the phase of the PTD signal and pump-probe offset is given by

$$m=\frac{1}{\mu_{\mathrm{s}}}=\left(\frac{\pi f}{\alpha_{\mathrm{s}}}\right)^{\frac{1}{2}}\ . \tag{6}$$

In practice the condition $a=b=z=0$ cannot be achieved. However, for the specimens with moderately high thermal diffusivity value, (6) holds well for finite values of $a$, $b$ and $z$ [17, 18]. A schematic of probe skimming is given in Fig. 1.

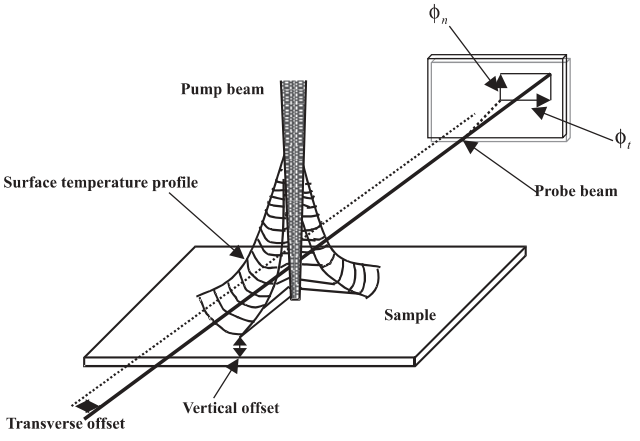


**FIGURE 1** Schematic diagram of the probe beam skimming PTD configuration; $y$, $z$, the transverse and vertical offsets respectively

## 3 Experimental

The samples used for the present studies are intrinsic InP and InP doped with Sn, S and Fe. The intrinsic InP has a carrier concentration of $10^{18}\,\mathrm{cm}^{-3}$. InP doped with Sn and S have a doping concentration of $10^{18}\,\mathrm{cm}^{-3}$ where as InP doped with Fe has a doping concentration of $10^{17}\,\mathrm{cm}^{-3}$. Measurements are done on the doped samples cleaved along (111) plane as well as (100) plane whereas the intrinsic sample is cleaved along (111) plane. All the samples have a thickness of $\sim 350\,\mu\mathrm{m}$ and are grown by epitaxial method.

Continuous optical radiation at 2.54 eV from an Argon ion laser (Liconix 5300), which is mechanically chopped (Stanford Research Systems SR 540) is used as the source of excitation. The laser beam has a Gaussian profile with a diameter of 1.2 mm. In all the measurements the power is kept at 50 mW (±0.5%) and the incident radiation is chopped at 15 Hz so that $\omega\tau \ll 1$. So only the thermal diffusion process contributes to the heat transport of the samples under investigation. The pump beam is focused using a convex lens having a focal length of 20 cm so as to get a spot size of 100 μm on the sample surface. Carbon tetra chloride ($CCl_4$) is used as the coupling liquid for the present investigation due to its high thermal diffusivity value ($\alpha = 0.731 \times 10^8\,\mathrm{cm^2\,s^{-1}}$) and the high rate of change of refractive index with temperature ($\mathrm{d}n/\mathrm{d}T = 6.12 \times 10^4\,\mathrm{K^{-1}}$) [20]. A 4 mW He-Ne laser (Uniphase) emitting at 633 nm is used as a probe beam to detect the strength of the refractive-index gradient in the $CCl_4$. The probe beam also has a Gaussian profile with a beam diameter of 700 μm and it is focused with a convex lens having a focal length of 8 cm to a spot size of 90 μm at the point of pump-probe crossing. The probe beam is arranged such that it just skims through the sample surface, and it propagates along the $y$ direction, which is orthogonal to the pump beam ($z$ axis). A position sensitive quadrant detector is used to measure the deflection of the probe beam. The output of the quadrant detector is fed to a dual phase lock-in amplifier (Stanford Research Systems SR 830). The entire experimental set up is laid out on a vibration-isolated table to protect the system from ambient vibrations. A schematic view of the experimental set up is shown in Fig. 2. In the present arrangement, the distance between the probe and the sample surface is kept as small as possible so as to get a nondiffracted beam (from the sample edge) at the detector head.

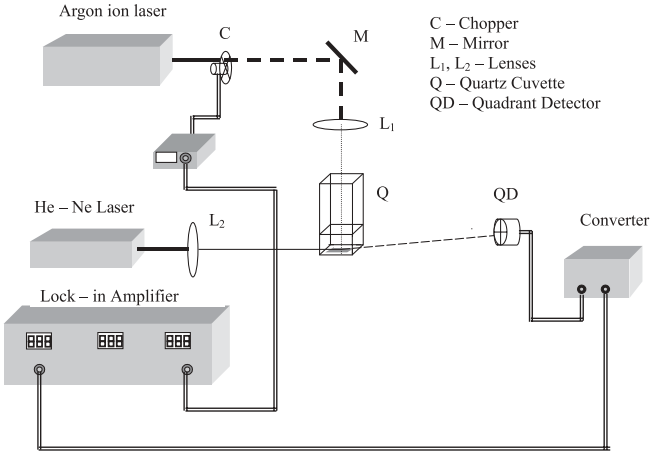


**FIGURE 2** Schematic view of the experimental set up

## 4 Results and discussion

Figure 3 shows the phase of PTD signal as a function of pump-probe offset for intrinsic InP cleaved at (111) plane. All other specimens under investigation also show similar behavior for the phase of PTD signal with respect to the pump-probe offset (not shown). The thermal diffusivity values are evaluated from the slope of the graph between PTD phase and pump-probe offset on either side of the point of excitation. The average value of the two measurements for all the specimens under investigation are tabulated in Table 1. It can be seen from the table that doped samples show a reduced value for thermal diffusivity compared to the intrinsic specimen. Although both the phonons and carriers can contribute to the heat transfer mechanism in semiconductors, for semiconductors having carrier concentrations less than $10^{20}\ \mathrm{cm^{-3}}$, the contribution from electrons to thermal conductivity ($k_e$) is negligibly small when compared to the contribution from phonons to the thermal conductivity ($k_e/k_{ph} = 10^{-3}$) [21, 22]. In the case of steady state photothermal experiments such as the photothermal deflection technique on semiconductors, the detected signal depends upon the thermal parameters (thermal diffusivity and thermal conductivity of both electrons and phonons) of each quasi particle as well as on the distribution of momentum and energy between them (which is generated through the nonradiative deexcitation of the specimen after illumination with chopped optical radiation). It has been reported earlier that for modulated photothermal experiments on semiconductors, for low chopping frequency range of incident radiation, as in the present case, the generation of the photothermal signal is essentially determined by the parameters of phonons alone [23]. The electronic thermal diffusivity of semiconductors is reported to be higher than that of phonon thermal diffusivity [11]. The measured thermal diffusivity value of all the samples under investigation

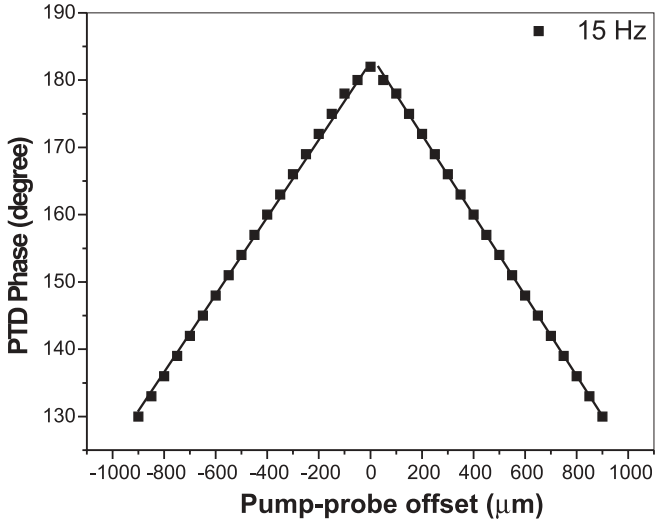


**FIGURE 3** Variation of PTD signal phase with pump-probe offset for intrinsic InP

| Sample | Plane of cleavage | Doping concentration | Thermal diffusivity ($\mathrm{cm^2\,s^{-1}}$) |
|---|---|---|---|
| InP | 111 | – | $0.438 \pm 0.003$ |
| InP: S | 111 | $10^{18}$ | $0.403 \pm 0.004$ |
| InP: S | 100 | $10^{18}$ | $0.394 \pm 0.003$ |
| InP: Sn | 111 | $10^{18}$ | $0.389 \pm 0.003$ |
| InP: Sn | 100 | $10^{18}$ | $0.382 \pm 0.002$ |
| InP: Fe | 111 | $10^{17}$ | $0.379 \pm 0.003$ |
| InP: Fe | 100 | $10^{17}$ | $0.360 \pm 0.004$ |

**TABLE 1** Thermal diffusivity of intrinsic and doped InP

agrees with the typical range of phonon thermal diffusivity in semiconductors [11]. In the case of semiconductors, the electron gas is heated by the surface and volume heat sources whereas phonon gas is heated by surface heat sources [11]. In the present case, all the semiconductor specimens under investigation are opaque at the incident wavelength (488 nm), so that heat sources are generated at the surface of the specimen. In the case of bulk semiconductors, the phonon energy relaxation takes place due to the diffusion of phonons alone and it is independent of the size of the specimen [22]. It can also be seen from the measured thermal diffusivity values that the interaction between electron and phonon is negligible. Otherwise, the measured thermal diffusivity should be the effective thermal diffusivity value of both electron thermal diffusivity and phonon thermal diffusivity [22]. In the case of semiconductors satisfying the condition $k_e/k_{ph} \sim 10^{-3}$, the contribution from electron diffusivity disappears in the phase of the dynamical part of phonon temperature [24]. Thus for all the samples under investigation it is the phonon assisted heat transport mechanism is the dominating mechanism in diffusion of thermal energy.

However, the propagation of phonons through the lattice suffers various scattering mechanisms such as phonon-phonon scattering, phonon-electron scattering, scattering from defects, scattering from boundaries etc. [25]. Phonon scattering is the key mechanism that limits the performance of both electronic and optoelectronic devices. The electron-phonon scattering mechanism is dominant only at very high carrier concentration. The boundary scattering mechanism in bulk semiconductors are dominant at low temperatures. The phonon-phonon scattering through normal (momentum conserving) and Umklapp processes and scattering from impurities are the key sources that are affecting the mean free path of phonons [25]. The lattice thermal conductivity of semiconductors is proportional to phonon mean free path and is given by the expression $k_{ph} = \frac{1}{3} C_v \nu l$, where $C_v$ is the thermal capacity per unit volume, $\nu$ is the sound velocity and $l$ is the phonon mean free path. Introduction of dopants into the lattice can result in disharmony in the periodic potential of the host lattice and thus can act as effective scattering centers for phonons. Thus the dopants in the lattice which act as point defects results in the scattering of phonons and this scattering mechanism is known as Rayleigh scattering and the corresponding scattering rate is given by the expression $\tau_{defect}^{-1} = A\omega^4$, where $\omega$ is the phonon angular frequency and $A$ is a constant related to the defect concentration [25]. Hence the introduction of dopants enhances the scattering rate and results in the reduction of mean free path of phonons and consequently a reduction in thermal conductivity. As the thermal diffusivity ($\alpha$) and thermal conductivity ($k$) are directly related to each other through the expression $\alpha = k/\varrho C$ (where $\varrho$ is the density and $C$ is the specific heat capacity) the reduction in one reduces the other. It is shown in [26] that lattice thermal conductivity $k$ is governed by lattice thermal resistivity ($W$) through the relation $k = 1/W = BT^q$, where $q$ is a constant at a particular temperature and $B$ is a parameter which decreases with increase in doping concentration. This also suggests that doping can result in a reduction in thermal conductivity (thermal diffusivity) of semiconductors.

It can also be seen the table that the Sn and S doped InP have higher thermal diffusivity value as compared to Fe doped semi insulating InP. The deep level impurity, which is usually a metal, is deliberately incorporated into the compound semiconductors to alter the device characteristics. Addition of controlled amounts of deep level impurities create midgap energy levels, which can act as recombination centers when there are excess carriers in the semiconductors and as generation centers when the carrier concentration is below its equilibrium value as in the reverse biased space region of $p$-$n$ junction or MOS capacitors [27]. Thus Fe doping results in midgap energy levels, which are known to create a large lattice relaxation around them, thereby acting as effective scattering centers for phonons [28]. As noted above, this increase in scattering centers reduces phonon mean free path and gives a reduced value for thermal diffusivity in Fe doped semi insulating InP.

In the case of InP doped with Sn and S, S doped InP shows a higher value for thermal diffusivity as compared to Sn doped InP. As pointed out earlier the scattering rate of phonons due to the impurities is given by the expression $\tau_{defect}^{-1} = A\omega^4$ in which $A$ is a doping concentration dependent parameter and is given by the expression

$$A = \frac{nV^2}{4\pi\nu_s^3}\left(\frac{\Delta M}{M}\right)^2 ,$$

where $n$ is the dopant concentration, $V$ is the volume of the host atom, $\nu_s$ is the average phonon group velocity, $M$ is the atomic mass of the host atom and $\Delta M$ is the mass difference between host atom and the impurity atom [25]. In the present investigation, the mass difference between Sn and P is greater than that of S and P and consequently phonons suffers a large scattering rate in Sn doped InP and hence show a reduced value for thermal diffusivity as compared to S doped InP.

From the table it is also obvious that the thermal diffusivity values of doped specimens cleaved in different planes are different. The plane of cleavage of compound semiconductors has great importance, especially in the fabrication of heterostructures. The difference in thermal diffusivity of the specimens cleaved along different planes can be understood in terms of variation in bond density with the plane of cleavage and phonon assisted heat transport in semiconductors. In the case of InP, the sample cleaved along (111) plane has an average distance between the cation and anion, whereas the samples cleaved along the (100) plane have a cation-anion distance of $d/\sqrt{3}$ [26]. Thus the bond density is high for the specimens cleaved in the (100) plane as compared to the samples cleaved in the (111) plane. In all the samples where the phonons are the major carriers of heat transport, the dynamic part of phonon temperature depends only on the characteristic features of phonons. As the bond density increases, the average phonon density also increases. The corresponding thermal diffusivity value $\alpha = k/\varrho C$ also decreases. Besides that, the decrease in cation-anion distance effectively reduces the phonon mean free path and consequently thermal diffusivity value as well. The phonon relaxation time also increases with decrease in bond density resulting in a reduced value for thermal diffusivity for the specimens cleaved along the (100) plane.

## 5 Conclusion

In this paper the thermal diffusivity values of intrinsic and doped samples of compound semiconductor InP cleaved along different planes was measured. From the analysis of data it is seen that the doping can influence the thermal diffusivity value through the scattering process of phonons. It is can also be seen from the analysis that the semi insulating Fe doped InP has a lower thermal diffusivity value as compared to Sn and S doped InP which in turn indicates that mid gap energy levels can influence the heat transport and hence thermal diffusivity value. Analysis of the data shows that thermal diffusivity value is sensitive to the direction of heat flow in semiconductor wafers. The current investigation clearly shows that in the case of semiconductors, which have carrier concentration less than $10^{20}\,\mathrm{cm}^{-3}$, the heat transport and hence thermal diffusivity value greatly depends on the propagation of phonons through the lattice.

**ACKNOWLEDGEMENTS** This work is supported by the Netherlands university federation for international collaboration (NUFFIC), the Netherlands under the MHO assistance to International School of Photonics. The authors also wish to acknowledge Prof. J.H. Wolter and Dr. J.E.M. Haverkort (COBRA Group, Technical University of Eindhoven, the Netherlands) for their constant encouragement as well as for providing the semiconductor samples used in this report. S.D. George acknowledges the Council of Scientific and Industrial Research, New Delhi for providing financial assistance. V.P.N. Nampoori also acknowledges the University Grant Commission for financial assistance through a research award project.

## REFERENCES

1 J. Singh: *Semiconductor Optoelectronics Physics and Technology* (Mc-Graw Hill 1995)
2 V. Mitin, V.A. Kochelap, M.A. Stroscio: *Quantum Hetrostructures Microelectronics and Optoelectronics* (Cambridge University Press 1999)
3 M. Soltanolkotabi, G.L. Bennis, R. Gupta: J. Appl. Phys. **85**(2), 794 (1999)
4 D. Fournier, V. Bocara, A. Skumanich, N.M. Amer: J. Appl. Phys. **59**, 787 (1986)
5 S.D. George, S. Dilna, P. Radhkrishnan, C.P.G. Vallabhan, V.P.N. Nampoori: Phys. Status Solidi (a) **195**(2), 416 (2003)
6 A. Mandelis (Ed.): *Photoacoustic and Thermal Wave Phenomena in semiconductors* (North-Holland, Amsterdam 1987)
7 A. Rosecwaig: *Photoacoustic and Photoacoustic Spectroscopy* (Wiley Interscience, New York 1983)
8 J.A. Sell (Ed.): *Photothermal Investigations of Solids and Fluids* (Acadamic, Boston 1989)
9 P.K. Kuo, M.J. Lin, C.B. Reys, L.D. Favro, R.L. Thomas, D.S. Kim, S. Zhang, L.J. Inglehart, D. Fournier. A.C. Boccara, N. Yacoubi: Can. J. Phys. **64**, 1165 (1986)
10 M. Bertolotti, R.L. Voti, G. Liakhou, C. Sibila: Rev. Sci. Instrum. **64**, 1576 (1993)
11 Yu.G. Gurevich, G. Gonzalez de la Cruz, G. Logvinov, M.N. Kasyanchuk: Semiconductors **32**(11), 1179 (1998)
12 P. Hess, J. Pelzl (Eds.): *Photoacoustic and Photothermal Phenomena* (Springer, Berlin 1988)
13 D. Bicanic (Ed.): *Photoacoustic and Photothermal Phenomena* III (Springer-Verlag, Berlin 1992)
14 W.B. Jackson, N.M. Amer, C. Boccara, D. Fournier: Appl. Optics **20**(8), 1333 (1981)
15 M. Bertolotti, G. Liakhou, R. Li Voti, A. Matera, C. Sibila, M. Valentino: Optical Eng. **36**(2), 515 (1997)
16 N.A. George, C.P.G. Vallabhan, V.P.N. Nampoori, P. Rahdakrishnan: Appl. Optics **41**(24), 5179 (2002)
17 A. Salzar, A.S. Lavega: Rev. Sci. Instrum. **65**, 2896 (1994)
18 A. Salzar, A.S. Lavega, J. Fernandez: J. Appl. Phys. **69**, 1216 (1991)
19 A. Mandelis, B.S.H. Royce: Appl. Optics **23**, 2892 (1984)
20 S.E. Bialkoswski: *Photothermal Spectroscopy Method Chemical Analysis* (Wiley, New York 1996)
21 G. Chen, C.L. Tien, X. Wu, J.S. Smith: J. Heat Transfer **116**, 325 (1994)
22 A.F. Sanchez, G. Gonzalez de la Cruz, Y. Gurevich, G.L. Logvinov: Phys. Rev. B **59**(16), 10 630 (1999)
23 A. Gonzalez de la Cruz, Y.G. Gurevich: Phys. Rev. B **58**(12), 7768 (1998)
24 A. Gonzalez de la Cruz, Y.G. Gurevich: J. Appl. Phys. **80**(3), 1726 (1996)
25 A.D. McConnell, U. Goodson: J. Micro-electromechan. Systems **10**(3), 360 (2001)
26 S. Adachi: *Physical Properties of III-V semiconductor compounds* (Wiley, New York 1992)
27 D.K. Schroder: *Semiconductor material and device characterisation* (Wiley, New York 1998)
28 S.D. George, C.P.G. Vallabhan, M. Heck, P. Radhakrishnan, V.P.N. Nampoori: J. Nondestructive Testing Evaluation **18**(2), 75 (2002)